J. CHEM. SOC. FARADAY TRANS., 1990, 86(4), 603–607

Mechanism of CuCl and CuO Chemiluminescence in Microwave-induced Plasma Afterglows at 300 K

Chris Vinckier,* Johan Corthouts and Stephan De Jaegere
Laboratory of Analytical and Inorganic Chemistry, K. U. Leuven, Celestijnenlaan 200F, 3030 Leuven, Belgium

The sublimation of the copper halides CuCl or $CuCl_2$ in microwave-induced plasma afterglows results in the chemiluminescence of CuCl at 300 K. In O_2–He afterglows the A, B, C, D, E and F transitions up from $v' = 3$ are observed, while H_2–He afterglows are much less effective, showing only A and B transitions. In addition, a weak chemiluminescence of CuO is detected in O_2–He afterglows. Various chemiluminescence mechanisms are discussed, from which it appears that the termolecular recombination of hydrogen or oxygen atoms, with CuCl or CuO acting as a third body, is the most plausible chemiexcitation mechanism.

It has been shown in our previous work that microwave-induced plasma (MIP) afterglows in hydrogen–inert-gas mixtures strongly enhance the atomization of metal compounds.[1–3] Owing to their chemical reactivity, these afterglows provide a source of metal atoms in the gas phase at relatively low temperature.[4] Ground-state hydrogen or oxygen atoms play a crucial role in these afterglows and are found to be the ultimate atomization precursors.[1] In the present work our attention will be focused on another interesting phenomenon occurring in MIP afterglows at room temperature. It is indeed seen that in these systems the generation of copper atoms in the gas phase is accompanied by a strong chemiluminescence of some copper compounds. In contrast to the atomization phenomenon, it is unexpected that the chemiluminescence intensities of copper(I) chloride are much stronger in O_2–He MIP afterglows than in H_2–He mixtures.

In the past the chemiexcitation of copper(I) chloride was investigated at high temperatures in flames;[6] this medium is well suited for the detection of halogens[7–9] in the presence of copper. Copper(I) chloride emission bands have also been observed in systems where thermally evaporated copper atoms were allowed to react with chlorine.[10,11]

However, up to now only very little information has been given on the possible reaction paths leading to these chemiluminescence phenomena. By comparing the various emission bands and intensities of copper(I) chloride in both hydrogen- and oxygen-containing MIP afterglows, qualitative arguments will be gathered for deriving the reaction mechanism which lies at the basis of the chemiluminescence observed. This task is much easier in MIP afterglows than in flame systems, since the chemical and physical characteristics of the former are well established.

Experimental

The experimental set-up, including the flow reactor and detection systems, have been described previously[4] and will only be briefly summarized here. A copper halide pellet, $CuCl_s$ or $CuCl_{2,s}$ is heated 16 cm upstream of the MIP gas inlet, and the gas-phase products $Cu_xCl_{x,g}$ are carried downstream towards the reaction zone. Here the $Cu_xCl_{x,g}$ compounds are allowed to react with the MIP afterglow products of H_2–He or O_2–He gas mixtures. In addition to the atomic absorption and mass-spectrometric equipment available for the detection of metal atoms and other gas-phase products, the optical system can easily be switched into the emission mode. The detection of the light emission in the wavelength range between 300 and 700 nm was carried out by a McPherson model 270 monochromator with a Hamamatsu R818 photon-multiplier. The emission intensities are expressed in relative units, with the value of the highest peak set equal to one hundred. However, the characteristics of this type of multiplier show a relatively constant sensitivity within 50% in the wavelength range of interest. All emission measurements occurred at a fixed distance 10.5 cm downstream of the MIP inlet, corresponding to a reaction time of *ca.* 45 ms.

Results

The experimental conditions used for the registration of the CuCl emission are summarized in table 1. For a fixed reactor pressure of 10 Torr* and a gas temperature of 300 K, the other parameters, such as the temperature of the $CuCl_s$ or $CuCl_{2,s}$ sample, the MIP mixture composition and microwave power, were selected to achieve maximum intensities. While the green emission became visible in the whole H_2–He afterglow region starting at a solid sample temperature of 510 K, a much stronger green–blue emission was observed at 450 K in O_2–He afterglows. When the solid temperature T_s was slightly increased, the emission intensity reached a maximum; fig. 1 shows an example of the emission spectrum with $CuCl_{2,s}$ at a temperature $T_s = 525$ K in an O_2–He afterglow. The emission spectra of copper (I) chloride are relatively well known,[6,12–14] and the assignment of the various transitions was made on the basis of spectroscopic data and constants found in the literature.[15,16] They include the electronic transitions $A \rightarrow X$, $B \rightarrow X$, $C \rightarrow X$, $D \rightarrow X$, $E \rightarrow X$ and $F \rightarrow X$ of the CuCl molecule and a few weak bands of CuO.

In table 2 the relative emission intensities in H_2–He and O_2–He afterglows are given using both $CuCl_s$ and $CuCl_{2,s}$ as

Table 1. Experimental conditions for the registration of the copper(I) chloride emission in H_2–He and O_2–He MIP afterglows

MPI	gas temperature, T_g/K	pressure, P_r/Torr	mixture composition	microwave power P_w/W	solid temperature, T_s/K
H_2–He	300	10	3% H_2	20	547
O_2–He	300	10	5% O_2	75	525

---

* 1 Torr = 101 325/760 Pa.

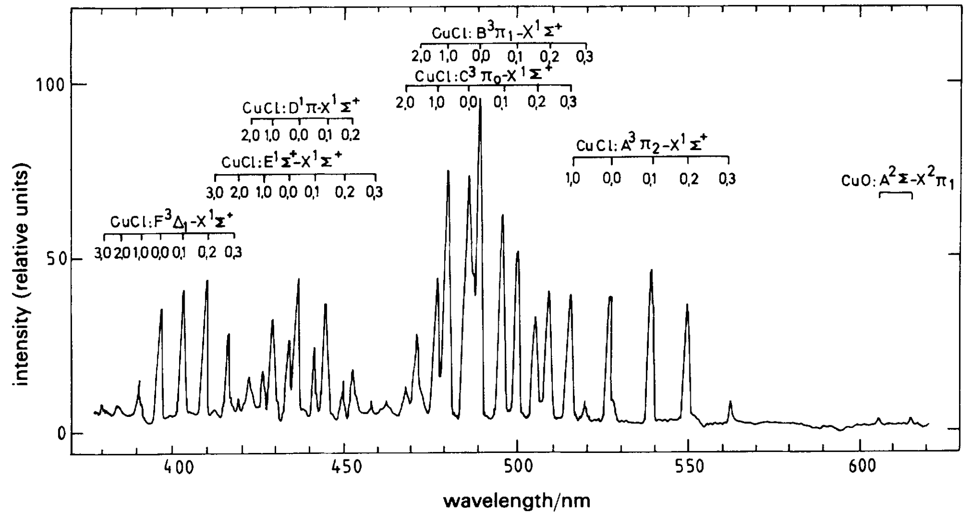

Fig. 1. Emission spectrum in a $CuCl_2$–O_2–He microwave-induced plasma afterglow. The experimental conditions are given in table 1.

solid samples. From the measurements it becomes immediately clear that the O_2–He MIP afterglow is a much more effective medium for the chemiexcitation of copper(I) chloride than is H_2–He. Although it is known that electronically excited helium atoms can provide a powerful source for the excitation of CuCl,[14] under our experimental conditions the emission completely vanished when either the H_2 or O_2 flows were turned off. This proves that, as is the case for the plasma

Table 2. Relative emission intensities of copper(I) chloride I_{CuCl*} in both H_2–He and O_2–He MIP afterglows (experimental conditions as table 1)

λ/nm			I_{CuCl*}			
			H_2–He		O_2–He	
obs	calc	transition	$CuCl_2$	CuCl	$CuCl_2$	CuCl
378.9	378.6	F $^3\Delta_1$–X $^1\Sigma^+$ (3, 0)	–	–	9.5	0.7
383.9	384.0	F $^3\Delta_1$–X $^1\Sigma^+$ (2, 0)	–	–	9.5	1.4
389.6	389.7	F $^3\Delta_1$–X $^1\Sigma^+$ (1, 0)	–	–	16.6	7.1
395.5	395.6	F $^3\Delta_1$–X $^1\Sigma^+$ (0, 0)	–	–	36.7	20.0
402.1	402.1	F $^3\Delta_1$–X $^1\Sigma^+$ (0, 1)	–	–	41.4	39.3
408.9	408.9	F $^3\Delta_1$–X $^1\Sigma^+$ (0, 2)	–	–	45.0	32.1
412.3	412.0	E $^1\Sigma^+$–X $^1\Sigma^+$ (3, 0)	–	–	8.9	0.7
415.7	415.8	F $^3\Delta_1$–X $^1\Sigma^+$ (0, 3)	–	–	30.2	12.9
418.9	418.8	E $^1\Sigma^+$–X $^1\Sigma^+$ (2, 0)	–	–	12.4	4.3
421.8	421.1	D $^1\Pi$–X $^1\Sigma^+$ (2, 0)	–	–	17.8	7.1
425.8	426.0	E $^1\Sigma^+$–X $^1\Sigma^+$ (1, 0)	–	–	19.5	5.7
428.5	428.1	D $^1\Pi$–X $^1\Sigma^+$ (1, 0)	–	–	34.3	13.6
433.1	433.2	E $^1\Sigma^+$–X $^1\Sigma^+$ (0, 0)	–	–	28.4	12.1
435.7	435.4	D $^1\Pi$–X $^1\Sigma^+$ (0, 0)	–	–	46.2	30.7
441.0	441.2	E $^1\Sigma^+$–X $^1\Sigma^+$ (0, 1)	–	–	27.2	12.1
443.9	443.4	D $^1\Pi$–X $^1\Sigma^+$ (0, 1)	–	–	39.1	24.3
449.3	449.4	E $^1\Sigma^+$–X $^1\Sigma^+$ (0, 2)	–	–	17.8	4.6
451.9	451.6	D $^1\Pi$–X $^1\Sigma^+$ (0, 2)	–	–	20.1	6.4
457.7	457.9	E $^1\Sigma^+$–X $^1\Sigma^+$ (0, 3)	–	–	11.8	1.4
461.6	461.5	B $^3\Pi_1$–X $^1\Sigma^+$ (3, 0)	–	–	11.8	1.4
467.3	467.0	C $^3\Pi_0$–X $^1\Sigma^+$ (2, 0)	–	–	15.4	2.1
471.0	470.0	B $^3\Pi_1$–X $^1\Sigma^+$ (2, 0)	–	–	30.2	12.1
475.7	475.6	C $^3\Pi_0$–X $^1\Sigma^+$ (1, 0)	–	–	46.2	31.4
479.2	478.9	B $^3\Pi_1$–X $^1\Sigma^+$ (1, 0)	–	–	76.3	38.6
484.7	484.7	C $^3\Pi_0$–X $^1\Sigma^+$ (0, 0)	–	–	74.0	35.0
488.3	488.2	B $^3\Pi_1$–X $^1\Sigma^+$ (0, 0)	0.7	–	100	89.3
495.0	494.6	C $^3\Pi_0$–X $^1\Sigma^+$ (0, 1)	–	–	62.7	26.4
	494.9	A $^3\Pi_2$–X $^1\Sigma^+$ (3, 0)				
498.4	498.2	B $^3\Pi_1$–X $^1\Sigma^+$ (0, 1)	0.7	–	51.3	82.9
505.8	503.9	C $^3\Pi_0$–X $^1\Sigma^+$ (0, 2)	–	–	36.0	26.2
	504.9	A $^3\Pi_2$–X $^1\Sigma^+$ (2, 0)				
509.0	508.8	B $^3\Pi_1$–X $^1\Sigma^+$ (0, 2)	0.7	0.6	42.7	37.1
515.5	515.2	A $^3\Pi_2$–X $^1\Sigma^+$ (1, 0)	0.6	0.7	41.3	37.1
519.5	519.5	B $^3\Pi_1$–X $^1\Sigma^+$ (0, 3)	–	–	11.3	2.9
526.3	526.2	A $^3\Pi_2$–X $^1\Sigma^+$ (0, 0)	4.3	0.7	40.7	23.9
538.1	538.0	A $^3\Pi_2$–X $^1\Sigma^+$ (0, 1)	3.6	0.7	48.0	66.4
550.0	550.1	A $^3\Pi_2$–X $^1\Sigma^+$ (0, 2)	0.7	–	38.5	33.6
562.5	562.9	A $^3\Pi_2$–X $^1\Sigma^+$ (0, 3)	–	–	12.4	3.2

Table 3. Relative emission intensities of copper oxide, I_{CuO^*} in O_2–He MIP afterglows (experimental conditions as table 1)

λ/nm			I_{CuO^*}	
obs	lit.	transition	$CuCl_2$	CuCl
522.7	524.0	D $^2\Delta_{5/2}$–X $^2\Pi_{3/2}$	–	2.5
530.3	531.2	C $^2\Pi_{1/2}$–X $^2\Pi_{3/2}$	–	1.8
605.5	605.9	A $^2\Sigma^-$–X $^2\Pi_{3/2}$	8.3	2.1
615.5	616.0	A $^2\Sigma^-$–X $^2\Pi_{1/2}$	8.3	2.9

afterglow atomization process, hydrogen and oxygen atoms are the key active afterglow components. The role of the metastable oxygen atoms $O(^1D)$ and $O(^1S)$ is completely negligible in these systems, in view of their very fast quenching rate with both atomic and molecular oxygen. This has quantitatively been discussed in some of our previous MIP afterglow studies.[1,4] The most striking phenomenon from table 2, however, is that the emission intensities are much stronger and at a higher energetic level in O_2–He MIP afterglows than in H_2–He mixtures. This was rather unexpected, since H_2–He afterglows are much more efficient atomization sources. From the measured absorbances in the same experimental conditions, a copper atom concentration of 2×10^{11} and 8×10^9 atom cm^{-3} could be calculated in, respectively, the H_2–He and O_2–He systems. While the atomization efficiency is about a factor of 25 lower, the chemiexcitation of O_2–He MIP afterglows is in many cases orders of magnitude higher. Qualitatively, the same situation is already been seen in flames. While only $A \rightarrow X$ and $B \rightarrow X$ transitions have been observed in rich hydrogen flames,[17] in addition the $C \rightarrow X$, $D \rightarrow X$ and $E \rightarrow X$ transitions are recorded in carbon monoxide flames. However, the presence of hydrogen or water reduces the CuCl emission intensity.[7] This has been explained by the removal of chlorine through reactions with hydrogen-containing species to form hydrochloric acid. Table 2 also shows that when $CuCl_{2,s}$ is used as a solid sample, slightly higher emission intensities are generally found, but the difference from $CuCl_s$ is relatively minor. This is not unexpected in view of the relatively easy conversion reaction

$$CuCl_{2,s} \rightarrow CuCl_s + \tfrac{1}{2}Cl_2$$

which starts at a sample temperature T_s of 470 K.[4] Note that the transitions from the states B to F all start from $v' = 3$ or 2. This can be explained by the occurrence of ω_e values of these excited states which are similar to those of ground-state CuCl and r_e values only shifted by 0.05 to 0.1 Å. While the $A \rightarrow X$ and $B \rightarrow X$ transitions of CuH* at, respectively, 428.9 and 380.4 nm[15,16] have not been observed in H_2–He MIP afterglows, a number of weak electronic transitions of CuO* are seen in O_2–He mixtures (table 3). However, contrary to the CuCl emission spectrum, no vibrational structure could be distinguished in the CuO* emission peaks. The assignment of the various bands is based on results from Delaval *et al.* for the electronic valence states and radiative lifetimes of CuO.[18]

Discussion

Chemical Composition of the MIP Afterglows containing Copper Halide

In order to clarify the reaction mechanism responsible for the MIP afterglow emission, a closer look must first be taken at the chemical composition of the afterglow region where a copper halide is being evaporated. By means of a mass-spectrometric detection system coupled directly to the reactor,[4] most of the species concentrations could be determined quantitatively. Stable products can be calibrated directly, while the concentrations of hydrogen and oxygen atoms were determined through the chemical titration technique with NO_2. The copper atom concentration was measured by atomic absorption spectroscopy. Only the concentrations of the other copper-containing compounds had to be calculated on the basis of the vapour pressures of the various copper halide oligomers[19,20] and the vaporization rate equation of Hertz-Knudsen-Langmuir as applied in our earlier work.[4] The results are shown in table 4. Concentrations with an index t_0 are given at reaction time $t = 0$, where the copper compounds in the gas phase are mixed with the MIP afterglow products, while the index t_1 refers to a position downstream of the mixing point at $t = 45$ ms. The various concentrations of Cu_xCl_x oligomers are taken the same for both CuCl and $CuCl_2$. This is acceptable on the basis of the rapid $CuCl_{2,s} \rightarrow CuCl_s + \tfrac{1}{2}Cl_2$ conversion, so that at least in the temperature range below 600 K, $[CuCl_{2,g}]$ remains completely negligible compared to $[Cu_xCl_{x,g}]$.[21] Note that the concentrations of the $Cu_xCl_{x,g}$ compounds are given at t = 0 ms: in this work no information is available on the concentrations of $Cu_xCl_{x,g}$ at $t = 45$ ms, where the luminescence spectra are recorded. Only in CuCl–H_2–He MIP afterglows does the amount of HCl formed indicate that at the utmost 18% of the initial $Cu_xCl_{x,g}$ has reacted. At these low levels the HCl concentration could only be determined within an error range of 30%. The major difference in the composition of the plasma afterglows starting from $CuCl_s$ or $CuCl_{2,s}$ lies in the large quantities of Cl_2 formed in the latter system. Additionally, a substantial amount of Cl_2 initially present is transformed to HCl in H_2–He MIP afterglows.

Table 4. Chemical composition of the MIP afterglows at the experimental conditions given in table 1

	H_2–He		O_2–He	
species[a]	$CuCl_s$	$CuCl_{2,s}$	$CuCl_s$	$CuCl_{2,s}$
$[H_2]_{t_0}$	9.6×10^{15}	9.6×10^{15}	–	–
$[H]_{t_0}$	1.5×10^{14}	1.5×10^{14}	–	–
$[O_2]_{t_0}$	–	–	1.6×10^{16}	1.6×10^{16}
$[O]_{t_0}$	–	–	9×10^{14}	9×10^{14}
$[CuCl_g]_{t_0}$	1.6×10^5	1.6×10^5	2×10^4	2×10^4
$[Cu_3Cl_{3,g}]_{t_0}$	2.8×10^{12}	2.8×10^{12}	6.8×10^{11}	6.8×10^{11}
$[Cu_4Cl_{4,g}]_{t_0}$	1.3×10^{12}	1.3×10^{12}	3×10^{11}	3×10^{11}
$[Cu_g]_{t_1}$	1.8×10^{11}	2.1×10^{11}	8.2×10^9	7.4×10^9
$[Cl_2]_{t_1}$	$<3 \times 10^{10}$	$<2.2 \times 10^{11}$	$<3 \times 10^{10}$	1.1×10^{12}
$[HCl]_{t_1}$	6.7×10^{11} [b]	2.3×10^{13} [b]	–	–

[a] The indices t_0 and t_1 refer to reaction times 0 and 45 ms, respectively (units are atom or molecule cm^{-3}). [b] ±30%.

Chemiexcitation Mechanism involving Ground-state Cu(^{2}S) Atoms

On the basis of the strong CuCl* luminescence observed in $Cu_g + Cl_2$ reaction systems,[10,11] one is tempted to put forwards the direct reaction

$$Cu_g + Cl_2 \rightarrow CuCl_g + Cl \quad \Delta H_{r,298} = -30 \text{ kcal mol}^{-1} \quad (1)$$

as a likely excitation source.* However, one must exclude reaction (1) on thermodynamic grounds. Indeed, the highest energetic transition F $^3\Delta_1$–X $^1\Sigma^+$(3, 0) lies at 378.9 nm (table 2), corresponding to an excitation energy of 74.9 kcal mol^{-1}. It is clear that reaction (1) cannot yield enough energy. This is *a fortiori* true for the CuO emission, where the endothermic reaction

$$Cu_g + O_2 \rightarrow CuO_g + O \quad \Delta H_{r,298} = 52.1 \text{ kcal mol}^{-1} \quad (2)$$

must certainly be rejected. Additionally, the energy threshold of 74.9 kcal mol^{-1} is a lower limit, since at a total pressure of 10 Torr vibration relaxation processes from upper states are likely to be fast.

Also, in view of the much higher Cl_2 content in $CuCl_2$–He than in CuCl–He MIP afterglows (table 4) one would expect a much stronger chemiluminescence of the former system which is not observed at all. This offers another qualitative argument against reaction (1) as the excitation source.

The direct combination of Cu atoms with Cl or O atoms though are energetically favourable:

$$Cu_g + Cl \xrightarrow{M} CuCl_g \quad \Delta H_{r,298} = -87.8 \text{ kcal mol}^{-1} \quad (3)$$

$$Cu_g + O \xrightarrow{M} CuO_g \quad \Delta H_{r,298} = -67.1 \text{ kcal mol}^{-1}. \quad (4)$$

For the CuCl excitation, reaction (3) has an excess energy of 12.9 kcal mol^{-1}, while for CuO the D $^2\Delta_{5/2}$–X $^2\Pi_{3/2}$ transition at 522.7 nm only requires 54.3 kcal mol^{-1}. Although this type of reaction is suggested to be responsible for the blue–green emission of CuCl in flames,[8,17] a number of arguments plead against these reactions in MIP afterglows.

First, the emission intensities in $CuCl_2$–H_2–He MIP afterglows are much weaker than in CuCl–O_2–He. If reaction (3) were the major reaction path one would expect the concentration product $[Cu_g][Cl_g]$ to be much lower in $CuCl_2$–H_2–He than in CuCl–O_2–He systems. On the contrary, as shown in table 4, $[Cu_g]$ is about a factor of 25 higher in $CuCl_2$–H_2–He MIP systems. Although the amount of atomic chlorine could not be measured in this work, one can at least make a rough estimation of its concentration. The excess amount of HCl produced in the $CuCl_2$–H_2–He system must be attributed to the fast reaction[22]

$$H + Cl_2 \rightarrow HCl + Cl \quad \Delta H_{r,298} = -45.3 \text{ kcal mol}^{-1}. \quad (5)$$

Since atomic chlorine is also formed in reaction (5) it is logical that atomic chlorine concentrations must also be higher in $CuCl_2$–H_2–He than in CuCl–O_2–He MIP afterglows. Thus the above consideration allows us to conclude that the concentration product $[Cu_g][Cl]$ should be higher in $CuCl_2$–H_2–He than in CuCl–O_2–He afterglows, and thus reaction (3) cannot be responsible for the observed chemiluminescence. A similar argument holds also in the same type of afterglow, where $CuCl_{2,s}$ must yield much higher chlorine atom concentrations than $CuCl_s$, while the emission intensities are of the same order of magnitude.

Secondly, the concentration ratio [O]/[Cl] in CuCl–O_2–He MIP afterglows exceeds 10^4, so that the production rate of CuO* in reaction (4) should be orders of magnitude larger than that of CuCl* in reaction (3). In view of the comparable lifetimes in the microsecond range of various CuO* and CuCl* electronically excited states,[13,23] one should see much stronger CuO* emission intensities; these are not observed under our experimental conditions.

Thirdly, it is established that the emission of CuH* bands in flames[23] are due to the reaction

$$Cu_g + H \xrightarrow{M} CuH_g \quad \Delta H_{r,298} = -64.9 \text{ kcal mol}^{-1}. \quad (6)$$

Although Cu_g and H are present in abundant quantities in H_2–He MIP afterglows, no CuH* bands are detected in our afterglow systems.

The foregoing offers conclusive evidence that the excitation mechanism comprising reactions (3) and (4), proposed to explain the emission of copper compounds in flames, cannot be important in our hydrogen- or oxygen-containing MIP afterglows at 300 K.

Chemiexcitation Mechanism involving Metastable Cu(^{2}D) Atoms

In a number of experiments, metastable electronically excited copper atoms Cu(^{2}D), when reacting with the halogens F_2, Cl_2 and Br_2, also showed chemiluminescence of the copper halides formed.[24,25] The following reactions can be written:

$$Cu(^2D_{5/2}) + Cl_2 \rightarrow CuCl_g + Cl \quad \Delta H_{r,298} = -61.8 \text{ kcal mol}^{-1} \quad (7)$$

$$Cu(^2D_{3/2}) + Cl_2 \rightarrow CuCl_g + Cl \quad \Delta H_{r,298} = -67.6 \text{ kcal mol}^{-1}. \quad (8)$$

Owing to the excitation energy of 11 203 and 13 245 cm^{-1} for, respectively, Cu($^2D_{5/2}$) and Cu($^2D_{3/2}$), reactions (7) and (8) are more exothermic than reaction (1) and are found to be responsible for the observed A, B, C → X transitions with $\Delta v \leqslant 3$ and for the D and E → X transitions from $v' = 0$, 1. However, in CuCl or $CuCl_2$–O_2–He MIP afterglows one also sees E and F → X transitions from $v' = 3$ (table 2), which are energetically not accessible at room temperature in reactions (7) and (8). Furthermore, if Cu(^{2}D) is formed in O_2–He systems, its concentration must be very low, since its quenching rate with O_2 must be very fast compared to the termolecular removal of ground-state Cu(^{2}S) atoms with O_2.[26] The same thermodynamic and kinetic arguments also hold for the role of Cu(^{2}D) in the copper oxide emission.

Chemiexcitation Mechanisms involving Molecular CuCl and CuO

The only possible excitation route remaining is a direct energization of molecular CuCl or CuO according to the following reaction sequence:

$$CuCl + 2H \rightarrow CuCl_g + H_2 \quad \Delta H_{r,298} = -104.2 \text{ kcal mol}^{-1} \quad (9)$$

$$CuCl + 2O \rightarrow CuCl_g + O_2 \quad \Delta H_{r,298} = -119.2 \text{ kcal mol}^{-1} \quad (10)$$

and

$$CuO + 2O \rightarrow CuO_g + O_2 \quad \Delta H_{r,298} = -119.2 \text{ kcal mol}^{-1}. \quad (11)$$

Reactions (9)–(11) can deliver enough excess energy for the observed chemiluminescence of both CuCl* and CuO*. The energy transfer from two recombining atoms to a third

---

* 1 cal = 4.184 J.

species has been invoked in the past to explain the strong chemiluminescence of the metals sodium, lead and thallium added to flames.[6,27] Also, the rate of production of $O(^1S)$ atoms through the recombination of two nitrogen or oxygen atoms with $O(^3P)$ acting as an energy captor has quantitatively been determined.[28] The direct excitation of $CuCl_g$ or CuO_g by hydrogen and oxygen atoms at least qualitatively explains the much stronger luminescence in O_2–He afterglows in view of the [O]/[H] ratio of *ca.* 6 and the square dependence on the atomic concentrations of reactions (9)–(11).

However, as shown in table 4, the achievable concentration of $CuCl_g$ through the vaporization of $CuCl_s$ or $CuCl_{2,s}$ is far too low to be responsible for this chemiluminescence process. This is *a fortiori* true for CuO_g, which is not present initially. Therefore a number of chemical reactions must first transform a fraction of the $Cu_xCl_{x,g}$ oligomers into $CuCl_g$ and CuO_g according to the following reaction sequence:

$$Cu_xCl_{x,g} + H, O, H_2, O_2 \rightarrow \cdots \rightarrow \cdots \rightarrow CuCl_g + \text{products} \quad (12)$$

$$Cu_xCl_{x,g} + O, O_2 \rightarrow \cdots \rightarrow \cdots \rightarrow CuO_g + \text{products} \quad (13)$$

followed by the excitation in reactions (9′)–(11′):

$$CuCl_g + 2H \rightarrow CuCl^* (A, B) + H_2 \quad (9')$$

$$CuCl_g + 2O \rightarrow CuCl^* (A, B, C, D, E, F) + O_2 \quad (10')$$

$$CuO_g + 2O \rightarrow CuO^* (A, C, D) + O_2. \quad (11')$$

This mechanism allows us to explain qualitatively a number of experimental observations: (1) Using $CuCl_s$ or $CuCl_{2,s}$ as a solid sample has no dramatic effect on the observed emission intensities, since the concentrations of the $Cu_xCl_{x,g}$ vaporization products of both copper halides are the same.[21] (2) The relative chemiluminescence efficiencies of H_2–He and O_2–He MIP afterglows can be explained by the fact that $[O]_{t_0} > [H]_{t_0}$. (3) In addition to the former argument, one expects a much lower $CuCl_g$ concentration in H_2–He MIP afterglows owing to the exothermic and probably fast removal of $CuCl_g$ by the reaction

$$CuCl_g + H \rightarrow Cu_g + HCl$$

$$\Delta H_{r,298} = -15.3 \text{ kcal mol}^{-1} \quad (14)$$

while the analogous process in O_2–He MIP afterglows must be unimportant owing to the endothermicity of the reaction

$$CuCl_g + O \rightarrow Cu_g + ClO \quad \Delta H_{r,298} = 23.5 \text{ kcal mol}^{-1}. \quad (15)$$

The above is confirmed by the fact that $[Cu_g]$ is much higher in H_2–He than in O_2–He MIP afterglows. (4) The relative weak CuO emission might be explained by a much lower concentration of CuO_g than of $CuCl_g$. Indeed, owing to its extremely low vapour pressure, CuO_g will quickly be removed from the reaction zone through wall loss.

While the foregoing arguments strongly support the experimental observations, further work must be carried out to substantiate the proposed excitation mechanism. In particular, the conversion of $Cu_xCl_{x,g}$ into $CuCl_g$ and CuO_g in reactions (12) and (13) must be investigated further. A kinetic modelling calculation is now under way to follow the concentration/time behaviour of all species mentioned in table 4. In this way it is hoped to establish a direct quantitative relationship between the chemiluminescence intensities and the MIP afterglow composition.

C.V. is a Research Director of the Belgian National Fund for Scientific Research. J.C. acknowledges a doctoral grant from the Belgian Institute for Scientific Research in Agriculture and Industry. We also thank the Fund for Joint Basic Research (F.K.F.O.) Belgium for a research grant.

References

1 S. De Jaegere, M. Willems and C. Vinckier, *J. Phys. Chem.*, 1982, **86**, 3569.

2 C. Vinckier, G. Stevens and S. De Jaegere, *React. Solids*, 1986, **1**, 275.

3 H. Brouwers and S. De Jaegere, *Spectrochim. Acta, Part B*, 1988, **43**, 1988.

4 (*a*) C. Vinckier, A. Dumoulin, J. Corthouts and S. De Jaegere, *J. Chem. Soc., Faraday Trans. 2*, 1988, **84**, 1725. (*b*) C. Vinckier, P. Coeckelberghs, G. Stevens, M. Heyns and S. De Jaegere, *J. Appl. Phys.*, 1987, **62**, 1450.

5 S. De Jaegere, M. Willems and C. Vinckier, *J. Phys. Chem.*, 1984, **88**, 259.

6 A. G. Gaydon, *The Spectroscopy of Flames* (Chapman and Hall, London, 2nd edn, 1974).

7 R. Mavrodineanu, *Analytical Flame Spectroscopy, Selected Topics* (Macmillan, London, 1970).

8 D. Marquardt, R. Stösser and H. Henrion, *Spectrochim. Acta, Part B*, 1981, **36**, 951.

9 D. F. Tomkins and C. W. Frank, *Anal. Chem.*, 1974, **46**, 1187.

10 G. A. Capelle, R. S. Bradford and H. P. Broida, *Chem. Phys. Lett.*, 1973, **21**, 418.

11 R. Rosenwaks, *Chem. Phys. Lett.*, 1979, **64**, 352.

12 P. R. Rao and K. K. Brody, *J. Chem. Phys.*, 1961, **35**, 776.

13 J. M. Delaval, Y. Lefebvre, H. Bocquet, P. Bernage and P. Niay, *Chem. Phys. Lett.*, 1987, **111**, 129.

14 P. Baltayan, J. C. Pebay-Peyroula and N. Sadeghi, *Chem. Phys. Lett.*, 1984, **104**, 168.

15 G. Hertzberg, *Molecular Spectra and Molecular Structure*, 1. *Spectra of Diatomic Molecules* (Van Nostrand, New York, 1950).

16 B. Rosen, *Selected Constants Relative to Diatomic Molecules* (Pergamon Press, New York, 1970).

17 Y. Tang and W. A. Aue, *J. Chromatogr.*, 1987, **408**, 69.

18 J. M. Delaval, F. David, Y. Lefebvre, P. Bernage, P. Niay and J. Schamps, *J. Mol. Spectrosc.*, 1983, **101**, 358.

19 M. Guido, G. Balducci, G. Gigli and M. Spoliti, *J. Chem. Phys.*, 1971, **55**, 4566.

20 *J. Phys. Chem. Ref. Data*, 1975, **4**, 1.

21 R. R. Hammer and N. W. Gregory, *J. Phys. Chem.*, 1964, **6**, 3229.

22 P. Bemand and M. A. Clyne, *J. Chem. Soc., Faraday Trans. 2*, 1977, **73**, 394.

23 E. M. Bulewicz and T. M. Sugden, *Trans. Faraday Soc.*, 1956, **52**, 1475.

24 R. W. Schwenz and J. M. Parson, *Chem. Phys. Lett.*, 1980, **71**, 524.

25 P. Baltayan, F. Hartman, J. C. Pebay-Peyroula and N. Sadeghi, *J. Phys. (Paris), Colloq. C7*, 1987, **4**, 573.

26 C. Vinckier, J. Corthouts and S. De Jaegere, *J. Chem. Soc., Faraday Trans. 2*, 1988, **84**, 1951.

27 R. Carabetta and W. Kaskan, *12th Int. Symp. Combustion* (Combustion Institute, Pittsburgh, 1967), p. 321.

28 R. A. Young and G. Black, *J. Chem. Phys.*, 1966, **44**, 3741.

Paper 9/03102B; *Received* 24*th July*, 1989